

Classical-quantum correspondence for inverted harmonic oscillator

Shangyun Wang^{1*}, Songbai Chen^{2,3†}, Jiliang Jing^{2,3 ‡}

¹*College of Physics and Electronic Engineering, Hengyang Normal University, Hengyang 421002, China*

²*Department of Physics, Key Laboratory of Low Dimensional Quantum Structures and Quantum Control of Ministry of Education, Synergetic Innovation Center for Quantum Effects and Applications,*

Hunan Normal University, Changsha, Hunan 410081, People's Republic of China

³*Center for Gravitation and Cosmology, College of Physical Science and Technology, Yangzhou University, Yangzhou 225009, People's Republic of China*

We investigate the classical-quantum correspondence in the inverted harmonic oscillator (IHO) system. It is shown that the out-of-time-order correlators (OTOCs) which the initial states are located at any position in the IHO system possess the same exponential growth rates (EGRs) as that at the saddle point, and their EGRs are twice the classical Lyapunov exponent (CLE) of the saddle point. Through the time evolution of mean photon number and the OTOCs, we exhibit that the classical-quantum correspondence in the IHO system not only depends on the initial system photon number, but also on the central positions of the initial states in the phase space. Moreover, we use the Husimi Q function to visualize the quantum wave packets during the OTOCs grow exponentially.

PACS numbers: 03.65.Ud, 03.67.Mn, 03.65.Aa

I. INTRODUCTION

The exponential growth behavior of OTOC has been regarded as a indicator of chaos or quantum instability in many quantum systems[1–16]. In particular, its growth rates are closely associated with the CLE λ in the large quantum numbers limit[12–15, 17–19]. In the context of black holes physics, the OTOC can be considered to as an indicator of chaos in gravity dual theory [20] and the corresponding upper bound of the maximum quantum Lyapunov exponent (QLE) is obtained in black hole geometry [1, 21, 22]. Experimentally, the OTOC has been measured in the ion traps systems[23–26] and in the nuclear magnetic resonance platforms[27–29].

However, an important discovery is that the OTOC in some non-chaotic regular systems also exhibit exponential growth behavior in early time, and the fast scrambling emerges not only in the chaotic case but also in the regular one[30, 31]. In the integrable systems, it is shown that the OTOCs in the vicinity of saddle points could grow exponentially since the quantum instability existing at saddle points [32]. The similar behavior of OTOC also appears in the inverted harmonic oscillator system with a Higgs potential[33]. It is not surprising because the instability of the saddle point causes its CLE to be positive. Then, it is natural to ask whether unstable regular orbits lead the OTOCs exhibit exponential growth behavior in early time. To study the early behavior of OTOC of unstable regular orbits, we consider the simplest unstable but regular system — the inverted

harmonic oscillator system, described by the Hamiltonian $\hat{H} = p^2/2m - m\omega^2 q^2/2$ [34]. This special system has been widely studied in various aspects. It is shown that this regular system has an exponential sensitivity to initial conditions as in the chaotic systems[35]. The phase-space volume of the classical inverted harmonic oscillator is unbounded, however, its corresponding volume for quantum inverted oscillator can be bounded by the system photons[36, 37]. Especially, the inverted harmonic oscillator is not just a pure theoretical model and has been realized experimentally[38]. In mathematics, it even challenges the Riemann hypothesis[39]. Moreover, it also shows important significance in both general relativity, quantum mechanics and chaotic domain[40–46].

Fidelity OTOC (FOTOC) is related to the quantum variance of Hermitian operators and provides a method for us to visualize the chaotic or scrambling dynamics of a quantum system in semi-classical phase space. Recently, it was shown to be associated with the CLE of chaotic systems[13, 15] and the quantum instability of saddle point in non-chaotic system [32]. In Schrodinger picture, the evolution of the quantum wave packets in the phase space are directly related to the quantum variance of momentum or coordinate operator. On the other hand, Husimi Q function is one of the quasi-probability distribution functions and was used to visualize the evolution of quantum wave packets in phase space[47–51]. In this paper, we study the early evolution of Husimi quasi-probability wave packets in IHO system and to see what Husimi quasi-probability wave packets behave as the OTOCs grow exponentially.

This paper is organized as follows. In section II, we study time evolution of mean photon number for different initial states in quantum IHO system. In section III, we analyze the early behavior of OTOCs for unstable orbits in IHO system and visualize the OTOCs by Husimi Q

*Corresponding author: sywang@hynu.edu.cn

†csb3752@hunnu.edu.cn

‡jljing@hunnu.edu.cn

function. Finally, we present results and a brief summary.

II. MEAN PHOTON NUMBER IN INVERTED HARMONIC OSCILLATOR

In this section, we study the classical one-dimensional IHO system with unstable regular orbits, namely,

$$H = \frac{p^2}{2m} + V, \quad V = -\frac{1}{2}m\omega^2 q^2, \quad (1)$$

where ω and m are the frequency and mass of IHO,

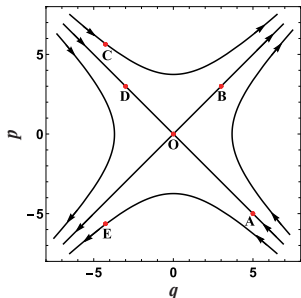


FIG. 1: The classical dynamics phase diagram of IHO. The coordinate (q, p) of points O, A, B, C, D and E are $(0, 0), (5, -5), (3, 3), (-4.267, 5.643), (-3, 3)$ and $(-4.267, -5.643)$, respectively. Point O is the saddle point.

respectively. In contrast to harmonic oscillator, the classical potential V tends to infinity in the limit $q \rightarrow \infty$. In Fig. 1, we present the classical dynamics phase diagram of IHO system. For the classical Hamiltonian (1), there is a saddle point $O(q = 0, p = 0)$ in phase space. For the particles on the asymptote ($p = -q$), they form a so-called stable manifold since these points move to the saddle point under the action of Hamiltonian (1). The particles starting from other positions move to infinity which forms an unstable manifold. It should be noted that all orbits in the IHO system are unstable, and the Lyapunov exponents are the same as the saddle point, i.e., $\lambda = 1$.

To study the quantum dynamics of IHO, we introduce the quadratic quantization form of the position and momentum operators and set $\hbar = m = \omega = 1$,

$$\hat{q} = (a^\dagger + a)/\sqrt{2}, \quad \hat{p} = i(a^\dagger - a)/\sqrt{2}, \quad (2)$$

then the quantum Hamiltonian of IHO becomes to

$$\hat{H} = -\frac{1}{2}(a^2 + a^{\dagger 2}). \quad (3)$$

Notice that the Hamiltonian (3) is equivalent to the Hamiltonian (1) in the classical limit when the system photon number $N_p \rightarrow \infty$. As in Refs.[48, 52], we take the photon coherent state as the initial state of system

$$|\psi\rangle = e^{-\beta\beta^*/2} e^{\beta a^\dagger} |0\rangle, \quad (4)$$

with

$$\beta = (q + ip)/\sqrt{2}. \quad (5)$$

where $|0\rangle$ is the ground state of light field, q and p are generalized coordinates and momentum. According to quantum theory, the mean photon number on the initial coherent state is

$$\langle a^\dagger a \rangle = \langle \psi | a^\dagger a | \psi \rangle = \beta\beta^\dagger = (q^2 + p^2)/2. \quad (6)$$

Eq.(6) implies that the mean photon number is related to the central position of coherent state in phase space. In other words, if the photon number of the system N_p is given, the coordinate and momentum parameters of coherent states in phase space are bounded in the region $(q^2 + p^2)/2 \leq N_p$. This shows that there is a natural boundary in phase space of the quantum IHO system with finite photon number, while the corresponding classical IHO system is unbounded.

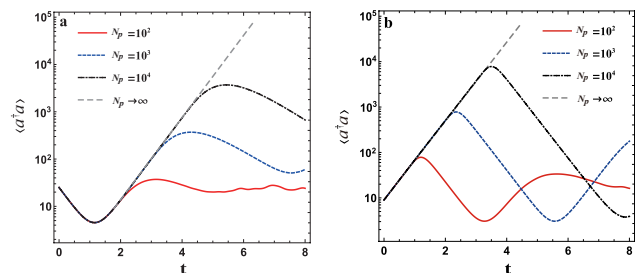


FIG. 2: Time evolution of the mean photon number for points A (a) and B (b) in Fig. 1 with different system photon number.

In Fig. 2, we show the time evolution of mean photon number $\langle a^\dagger a \rangle$ for points A and B with fixed system photon number. It's shown that the starting point located in the stable manifold of IHO, such as point A , the mean photon number $\langle a^\dagger a \rangle$ decreases firstly and then increases to the maximum value, as shown in Fig. 2(a). For the points far away from the saddle point under the action of Hamiltonian, such as point B , the mean photon number grows to the maximum value directly, as shown in Fig. 2(b). Whatever the center of the initial wave packets are located, the mean photon number $\langle a^\dagger a \rangle$ increases to infinity in the classical limit case $N_p \rightarrow \infty$. For the case with finite initial photon number N_p , the curve of mean photon number changing with time first overlaps that in the classical limit. After a time t_p , the increase of mean photon number are no longer consistent with that in the classical limit case. This means that during the period $0 < t \leq t_p$ there exists the so-called classical-quantum correspondence for the system (1) because as $t > t_p$ the quantum behavior in the system differs from that in the classical system. We also note that the time t_p increases with the initial photon number N_p , which is understandable because the classical-quantum correspondence becomes clearer in the system with larger photon

number. Moreover, the time t_p for maintaining the classical quantum correspondence is less than the time which the mean number of photon increases to its maximum value. Strictly speaking, the time to maintain the classical quantum correspondence in IHO system is not given by the maximum of mean photon number.

Comparing Figures 2(a) and 2(b), for fixed initial photon number N_p , we find that the time to maintain the classical quantum correspondence for the initial coherent state centred at point A is longer than that at point B . It implies that the length of time maintaining classical-quantum correspondence in the quantum IHO depends on the central positions of the initial coherent states of system in the phase space.

III. EXPONENTIAL GROWTH OF OTOC IN INVERTED HARMONIC OSCILLATOR

In this section, we study the quantum variance derived from the OTOC in the IHO system and analyse the Husimi quasi-probability wave packet during the OTOC growth exponentially. The OTOC is defined as[54]

$$C(t) = \langle [\hat{W}(t), \hat{V}(0)]^\dagger [\hat{W}(t), \hat{V}(0)] \rangle, \quad (7)$$

where $\langle \dots \rangle$ denotes the expectation values and $\hat{W}(t) = e^{i\hat{H}t}\hat{W}e^{-i\hat{H}t}$. \hat{H} is a quantum Hamiltonian, \hat{W} and \hat{V} are two arbitrary local operators. Here, we choose $\hat{W} =$

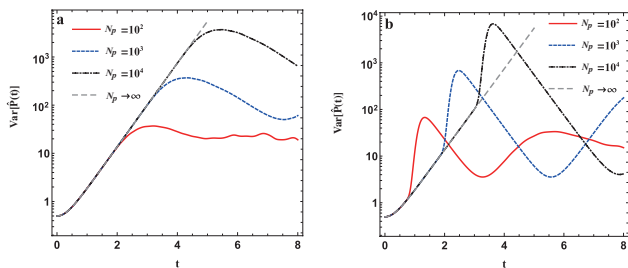


FIG. 3: Time evolution of the OTOC for point A (a) and B (b) in Fig. 1 with different system photon number.

$\hat{P} = i(a^\dagger - a)/\sqrt{2}$ and \hat{V} as a projection operator onto the initial state $|\psi\rangle$, i.e., $\hat{V} = |\psi\rangle\langle\psi|$. Substituting the operators $\hat{V} = |\psi\rangle\langle\psi|$ and $\hat{W} = \hat{P}$ into the Eq. (7), one has

$$C(t) = \langle \psi(t) | \hat{P}^2 | \psi(t) \rangle - \langle \psi(t) | \hat{P} | \psi(t) \rangle^2 \quad (8)$$

$$\equiv \text{Var}[\hat{P}(t)], \quad (9)$$

where $\text{Var}[\hat{P}(t)]$ is the quantum variance of the momentum operator \hat{P} . This relation is similar to the definition of FOTOC[13] and enable us to visualize the OTOC in semiclassical phase space. Figures 3(a) and 3(b) show that the EGRs $\tilde{\lambda}$ of OTOC are independent of system photon number N_p and the central positions of initial

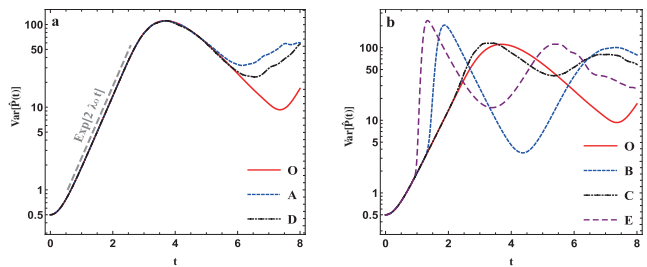


FIG. 4: Time evolution of the OTOC for the initial coherent states centered at different points. The gray dashed line in the left panel corresponds to the exponential growth rate given by twice the classical Lyapunov exponent. Here, we set the system photon number $N_p = 300$.

coherent states, and the time to keep $\text{Var}[\hat{P}(t)]$ growing exponentially increases with N_p .

For the initial states centered at the points in the stable manifold, the evolution of OTOCs are completely consistent before the Ehrenfest time $\tau = \frac{1}{\tilde{\lambda}} \ln N_p$, and the EGRs are twice the CLE of saddle point, i.e $\tilde{\lambda} = 2\lambda_O$, as shown in Fig. 4(a). In Fig. 4(b), we find that the time of the OTOC owning the same EGR as the saddle point depends on the central positions of the initial state in the phase space. From the view of the evolution of the OTOC, Figs. 3 and 4(b) further illustrate that both the photon number of system and the central positions of the initial coherent states affect the classical-quantum correspondence in the IHO system.

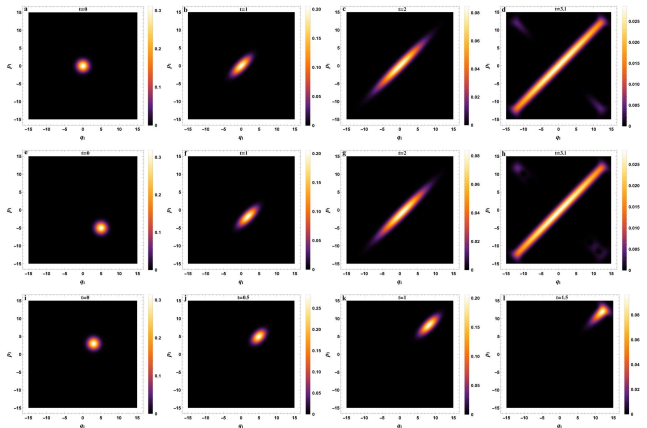


FIG. 5: Change of Husimi quasi-probabilistic wave packets with time for fixed system photon number $N_p = 300$. The top, middle and bottom panels denote respectively the case in which the initial coherent state centered at the points O , A and B in Fig. 1.

Husimi Q function is one of the quasi-probability distribution functions, and it was used to distinguish chaotic and periodic orbits in quantum systems[47–52]. The def-

inition of Husimi Q function is

$$Q(q_1, p_1) = \frac{1}{\pi} \langle q_1, p_1 | \rho | q_1, p_1 \rangle, \quad (10)$$

where $|q_1, p_1\rangle$ is photon coherent state and ρ is the density matrix. In Fig. 5, we present the change of Husimi Q distribution in phase space for the IHO system with different initial values. Figures. 5(a)-5(c) and 5(e)-5(g) show that the change of quasi-probability wave packets for the initial points in the stable manifold own similar behaviors during the OTOC grows exponentially. This means that the evolution of OTOC associated with the initial states centre on stable manifold are highly consistent before the Ehrenfest time, which is also shown in Fig. 4(a). In Figs. 5(i)-5(l), we show that the evolution of Husimi quasi-probabilistic wave packet with the initial state centered at point B located on the unstable manifold. It is found that the time reduces for the wave packet owning the behaviors similar to that on stable manifold. During the OTOC grows exponentially, it is easy to found that in the IHO system, the corresponding quantum wave packets spread along the phase trajectory in the classical phase space. Especially, we note that the evolution of quasi-probability wave packets are identical except for the position during the OTOCs grow exponentially, as shown in Figs. 5(b), 5(g) and 5(k). In addition, we present the Husimi quasi-probabilistic wave packets after the OTOC grows exponentially in Figs. 5(d), 5(h) and 5(l) for points O, A and B . We find that some discrete wave packets appear outside the primary wave packet and there is no the corresponding classical states, which is different from those during the OTOC exhibits exponential growth behavior.

IV. CONCLUSION

In this article, we investigated the classical-quantum correspondence in the IHO system through the time evolution of mean photon number and OTOC. We show that both the system photon number and the central position of the initial coherent states affect the classical-quantum correspondence relationship in IHO system. For the starting points located in the stable manifold of IHO, the mean photon number decrease firstly and then increase to the maximum value, and the time evolution of OTOCs are completely consistent before the Ehrenfest time. For the points far away from the saddle point under the action of Hamiltonian, the mean photon number grow to the maximum value directly, and the time for the OTOCs maintaining exponential growth are depend on the central position of initial wave packets. Moreover, we exhibit that the EGRs of OTOCs at any position in the IHO system are twice the CLE of the saddle point. We analyze the Husimi quasi-probability wave packets of different initial states, and find that during the OTOC grows exponentially, the evolution of quasi-probability wave packets are identical except for the position. Our results could help to further understand the OTOC and correspondence principle.

V. ACKNOWLEDGMENTS

-
- [1] S. H. Shenker and D. Stanford, Black holes and the butterfly effect, *J. High Energy Phys.* 03 (2014) 067.
 - [2] D. A. Roberts and D. Stanford, Diagnosing Chaos Using Four-Point Functions in Two-Dimensional Conformal Field Theory, *Phys. Rev. Lett.* 115, 131603 (2015).
 - [3] E. R. Castro et al, Quantum-classical correspondence of a system of interacting bosons in a triple-well potential, *Quantum* 5, 563 (2021).
 - [4] M. Rautenberg and M. Gärttner, Classical and quantum chaos in a three-mode bosonic system, *Phys. Rev. A* 101, 053604 (2020).
 - [5] B. Craps et al, Lyapunov growth in quantum spin chains, *Phys. Rev. B* 101, 174313 (2020).
 - [6] R. K. Shukla, A. Lakshminarayan, and S. K. Mishra, Out-of-time-order correlators of nonlocal block-spin and random observables in integrable and nonintegrable spin chains, *Phys. Rev. B* 105, 224307 (2022).
 - [7] M. McGinley, A. Nunnenkamp, and J. Knolle, Slow Growth of Out-of-Time-Order Correlators and Entanglement Entropy in Integrable Disordered Systems, *Phys. Rev. Lett.* 122, 020603 (2019).
 - [8] T. Akutagawa, K. Hashimoto, T. Sasaki, and Ryota Watanabe, Out-of-time-order correlator in coupled harmonic oscillators, *J. High Energy Phys.* 08 (2020) 013.
 - [9] E. M. Fortes et al, Gauging classical and quantum integrability through out-of-time-ordered correlators, *Phys. Rev. E* 100, 042201 (2019).
 - [10] R. K. Shukla, A. Lakshminarayan, and S. K. Mishra, Out-of-time-order correlators of nonlocal block-spin and random observables in integrable and nonintegrable spin chains, *Phys. Rev. B* 105 224307 (2022).
 - [11] M. McGinley, A. Nunnenkamp, and J. Knolle, Slow Growth of Out-of-Time-Order Correlators and Entanglement Entropy in Integrable Disordered Systems, *Phys. Rev. Lett.* 122, 020603 (2019).
 - [12] K. Hashimoto, K. Muratab, and R. Yoshii, Out-of-time-order correlators in quantum mechanics, *J. High Energy Phys.* 10 (2017) 138.
 - [13] R. J. Lewis-Swan, A. Safavi-Naini, J. J. Bollinger, and A. M. Rey, Unifying scrambling, thermalization and entanglement through measurement of fidelity out-of-time-order correlators in the Dicke model, *Nat. Commun.* 10, 1581 (2019).
 - [14] J. Chávez-Carlos et al, Quantum and Classical Lyapunov Exponents in Atom-Field Interaction Systems, *Phys. Rev. Lett.* 122, 024101 (2019).

- [15] A. V. Kirkova, D. Porras, and P. A. Ivanov, Out-of-time-order correlator in the quantum Rabi model, *Phys. Rev. A* 105, 032444 (2022).
- [16] J. Wang, G. Benenti, G. Casati, and W. Wang, OQuantum chaos and the correspondence principle, *Phys. Rev. E* 103, L030201 (2021).
- [17] S. H. Shenker and D. Stanford, Black holes and the butterfly effect, *J. High Energy Phys.* 03 (2014) 067.
- [18] A. Bohrdt, C. B. Mendl, M. Endres, and M. Knap, Scrambling and thermalization in a diffusive quantum many-body system, *New J. Phys.* 19, 063001 (2017).
- [19] H. Shen, P. Zhang, R. Fan, and H. Zhai, Out-of-time-order correlation at a quantum phase transition, *Phys. Rev. B* 96, 054503 (2017).
- [20] J. M. Maldacena, The Large N limit of superconformal field theories and supergravity, *Int. J. Theor. Phys.* 38 (1999) 1113.
- [21] S.H. Shenker and D. Stanford, Multiple shocks, *J. High Energy Phys.* 12 (2014) 046.
- [22] J. Maldacena, S.H. Shenker, and D. Stanford, A bound on chaos, *J. High Energy Phys.* 08 (2016) 106.
- [23] M. Gärttner, J. G. Bohnet et al, Measuring out-of-time-order correlations and multiple quantum spectra in a trapped-ion quantum magnet, *Nat. Phys.* 13, 781 (2017).
- [24] K. A. Landsman, C. Figgitt et al, Verified quantum information scrambling, *Nature (London)* 567, 61 (2019).
- [25] M. K. Joshi, A. Elben et al, Quantum Information Scrambling in a Trapped-Ion Quantum Simulator with Tunable Range Interactions, *Phys. Rev. Lett.* 124, 240505 (2020).
- [26] A. M. Green, A. Elben et al, Experimental measurement of out-of-time-ordered correlators at finite temperature, *Phys. Rev. Lett.* 128, 140601 (2022).
- [27] J. Li, R. Fan, H. Wang, B. Ye, B. Zeng, H. Zhai, X. Peng, and J. Du, Measuring Out-of-Time-Order Correlators on a Nuclear Magnetic Resonance Quantum Simulator, *Phys. Rev. X* 7, 031011 (2017).
- [28] K. X. Wei, C. Ramanathan, and P. Cappellaro, Exploring Localization in Nuclear Spin Chains, *Phys. Rev. Lett.* 120, 070501 (2018).
- [29] M. Niknam, L. F. Santos, and D. G. Cory, Sensitivity of quantum information to environment perturbations measured with a nonlocal out-of-time-order correlation function, *Phys. Rev. Research* 2, 013200 (2020).
- [30] B. Bhattacharjee, X. Cao, P. Nandy, and T. Pathak . Krylov complexity in saddle-dominated scrambling. *J. High Energy Phys.* 2022, 174 (2022).
- [31] T. Xu, T. Scaffidi, and X. Cao, Does Scrambling Equal Chaos?, *Phys. Rev. Lett.* 124, 140602 (2020).
- [32] Saúl Pilatowsky-Cameo et al, Positive quantum Lyapunov exponents in experimental systems with a regular classical limit, *Phys. Rev. E* 101, 010202(R) (2020).
- [33] K. Hashimoto, K. Huh, K. Kimb, and R. Watanabea, Exponential growth of out-of-time-order correlator without chaos: inverted harmonic oscillator, *J. High Energy Phys.* 11 (2020) 068.
- [34] G. Barton, Quantum mechanics of the inverted oscillator, *Ann. Phys. (N.Y.)* 166, 322 (1986).
- [35] R. Blume-Kohout and W. Zurek, Decoherence from a chaotic environment: An upside-down oscillator as a model, *Phys. Rev. A* 68, 032104 (2003).
- [36] K. Gietka, T. Busch, Inverted harmonic oscillator dynamics of the nonequilibrium phase transition in the Dicke model, *Phys. Rev. E* 104, 034132 (2021).
- [37] K. Gietka, Squeezing by critical speeding up: Applications in quantum metrology, *Phys. Rev. A* 105, 042620 (2022).
- [38] S. Gentilini, M. C. Braidotti, G. Marcucci, E. DelRe, and C. Conti, Physical realization of the Glauber quantum oscillator, *Sci. Rep.* 5, 15816 (2015).
- [39] M. V. Berry and J. P. Keating, The Riemann zeros and eigenvalue asymptotics, *SIAM Rev.* 41, 236 (1999).
- [40] S. Choudhury et al, Four-mode squeezed states in de Sitter space: A study with two field interacting quantum system, arXiv:2203.15815.
- [41] L. Qu, J. Chen, Y. Liu, Chaos and Complexity for Inverted Harmonic Oscillators, *Phys. Rev. D* 105, 126015 (2022).
- [42] V. Subramanyan et al, Physics of the Inverted Harmonic Oscillator: From the lowest Landau level to event horizons, *Annals of Physics* 435 (2021) 168470.
- [43] Z. Tian et al, Verifying the upper bound on the speed of scrambling with the analogue Hawking radiation of trapped ions, *Eur. Phys. J. C* 82, 212 (2022).
- [44] Z. Lewis and T. Takeuchi, Position and Momentum Uncertainties of the Normal and Inverted Harmonic Oscillators under the Minimal Length Uncertainty Relation, *Phys. Rev. D* 84, 105029 (2011).
- [45] P. Betzios, N. Gaddam, and O. Papadoulaki, Black holes, quantum chaos, and the Riemann hypothesis, *SciPost Phys. Core* 4, 032 (2021).
- [46] T. Morita, Thermal Emission from Semiclassical Dynamical Systems, *Phys. Rev. Lett.* 122, 101603 (2019).
- [47] K. Takahashi and N. Saitô, Chaos and Husimi Distribution Function in Quantum Mechanics, *Phys. Rev. Lett.* 55, 645 (1985).
- [48] S. Wang, S. Chen and J. Jing, Effect of system energy on quantum signatures of chaos in the two-photon Dicke model, *Phys. Rev. E* 100, 022207 (2019).
- [49] S. Chaudhury, A. Smith, B. E. Anderson, S. Ghose and P. S. Jessen, Quantum signatures of chaos in a kicked top, *Nature (London)* 461, 768 (2009).
- [50] A. Piga, M. Lewenstein and J. Q. Quach, Quantum chaos and entanglement in ergodic and nonergodic systems, *Phys. Rev. E* 99, 032213 (2019).
- [51] V. Mourik et al, Exploring quantum chaos with a single nuclear spin, *Phys. Rev. E* 98, 042206 (2018).
- [52] K. Furuya, M. C. Nemes, and G. Q. Pellegrino, Quantum Dynamical Manifestation of Chaotic Behavior in the Process of Entanglement, *Phys. Rev. Lett.* 80, 5534(1998).
- [53] See Supplemental Material at <http://link.aps.org/supplemental/10.1103/PhysRevE.101.010202> for details.
- [54] A. I. Larkin and Yu. N. Ovchinnikov, *Zh. Eksp. Teor. Fiz.* 55, 2262 (1969) [*Sov. Phys. JETP* 28, 1200 (1969)].
- [55] J. Chávez-Carlos, Classical chaos in atom-field systems. *Phys. Rev. E* 94, 022209 (2016).

